**Educational Administration: Theory and Practice**
2024, 30(6), 380-393
ISSN: 2148-2403
https://kuey.net/

**Research Article**

# Numerical study of thermal comfort in buildings designed with local building materials in humid tropical climate zones

Kokou Dowou[1], Yawovi Nougbléga[1,2*], Komi Apélete Amou[2,3]

[1]Laboratoire Sur l'Energie Solaire /Groupe Phénomène de Transfert et Energétique, Université de Lomé, 01 Lomé, BP 1515.
[2*]Regional Centre of Excellence on Electricity Management (CERME), University of Lomé
[3]Laboratoire Sur l'Energie Solaire, Département de Physique, Faculté Des Sciences (FDS), Université de Lomé, 01 Lomé, BP 1515.

**Citation:** Yawovi Nougbléga, at al (2024), Numerical study of thermal comfort in buildings designed with local building materials in humid tropical climate zones, Educational Administration: Theory and Practice, 30(6), 380-393
Doi: 10.53555/kuey.v30i6.5206

**ARTICLE INFO**

**ABSTRACT**

Bioclimatic building, which consumes less energy, appears to be the answer both to reduce electricity consumption for air conditioning and lighting and to protect the environment. Nowadays, it is essential to develop construction systems based on locally available building materials in the design of building walls and roofs. This study aims to promote the construction of energy-efficient housing using environmentally friendly local materials and provide thermal comfort for occupants. A comparative study of thermal comfort achieved in buildings designed based on the combination of various local building materials in the wall and lightweight roof envelopes is carried out by numerical investigation. Energy equations written by the nodal method on the walls and roof, discretized by the finite difference method, are solved by the iterative Gauss-Seidel method. The indoor air temperatures of the different building types are simulated and the thermal responses of the envelopes are analyzed. The results presented in terms of thermal comfort in buildings constructed using the proposed local materials show that Typha is a naturally insulating material which offers excellent protection against the heat in hot or cold periods in the building. The introduction of insulation plant fibre reduces significantly to 6°C the temperature inside the building.

**Keywords**: Numerical simulation, construction systems, thermal comfort, local building materials

## 1. INTRODUCTION

Forecasts of the impact of climate change on buildings between 2030 and 2050 predict an increase in the frequency and intensity of heat waves (OIF,2015). At the same time, rapid population growth, the concentration of urban areas and the ageing of the population will lead to an increase in the number of vulnerable people (IFDD,2015). In sub-Saharan Africa, the urbanization rate, around 30% at the start of the 1990s, could rise to 50% by 2030. Therefore, an urgent need is to adopt a long-term dynamic aimed at implementing eco-responsible approaches in the design and refurbishment of buildings to improve their energy performance while reducing their carbon footprint as much as possible (Betti et al., 2024; Ullah et al., 2024). This means taking energy efficiency (Lawson,2005) into account in buildings, but also using eco-materials, taking into account their grey energy (Jannot, 1994). The constructional qualities of materials are decisive selection criteria, as are their cost, lifespan, maintenance requirements, market availability and aesthetic appeal (Jannot, 1994). Added to this are the environmental constraints of reducing their ecological footprint. The promotion of traditional local materials is an avenue worth exploring (Samah et al., 2022) as long as they limit transport needs and promote the local economy since their production process often requires low energy requirements through the use of simple techniques (Allouhi et al., 2015) The building sector is now one of the world's top three energy consumers, alongside the transport and industrial sectors (Jannot, 1994). The building sector consumes 40% of the world's energy (Cheung et al., 2004), and 50% of this annual consumption is generally caused by heating, ventilation and air conditioning systems (Cheung et al., 2004). This consumption, which is increasing energy costs, and with the negative consequences of greenhouse gas

emissions, it has become essential to develop innovative systems to improve energy efficiency, better control energy demand and reduce $CO_2$ emissions (Camara et al., 2018). This solution approach is helpful, as it is now imperative to use more sustainable local materials, solutions, methods and processes for a better future for the planet Earth (Boukli Hacene et al., 2011). A common theme among effective building design strategies is improving the thermal mass of the building envelope to store thermal energy during the day and return it to the building during the cooler night (Kaboré, 2020). This can reduce peak temperatures and temperature fluctuations inside the home (Aek, 2017). Improving indoor temperatures is a major economic and environmental challenge for the building industry (Cheung et al., 2004). Hence, the thermal mass conception of the building envelope to store thermal energy during the day and return it to the building during the cooler night (Jannot, 1994) is promising. For all these reasons, new buildings should be designed to be energy-efficient, use local materials, be sufficiently resilient to adapt to climate change (Guiavarch Alain, 2003) and offer better thermal comfort (Camara et al., 2022). The building design is based primarily on energy-saving criteria, combining insulation, solar gain, inertia and thermal comfort (Boukli Hacene et al., 2011). The type of building envelope has a profound effect on its thermal behaviour. Dried earth block construction offers good thermal performance compared with cement breeze block buildings, with 40 to 60% compared with 10 to 40% relative to humidity, and a temperature of 24°C compared with 29°C, respectively (Maamar, 2019). (Dalel, 2010) carried out a study on the impact of thermal insulation on the interior temperature of a building and concluded that the use of insulation allows a significant lowering of the interior temperature with the air space and that its location is on the thermal mass side (Medjelakh et al., 2008). (Dalila Benamara et al., 2010) have developed a high-performance slab based on locally available and carefully researched materials. A great deal of work has focused on the use of plant reinforcements such as bamboo and rattan in concrete (Fezzioui et al., 2018). All the authors agree that the design equations and procedures for steel-reinforced concrete can be safely applied to the design of bamboo-reinforced concrete beams (Gbaguidi et al., 2011). (Kachkouch, S., 2019) studied the thermal and energy performance of a prototype classroom building in a rural area in Marrakech, Morocco. The author made a comparison between the building using concrete block walls and the one using stabilized rammed earth walls. His results showed that the high inertia of the stabilized rammed earth walls made it possible to stabilize the operating temperature throughout the year, resulting in a reduction in annual requirements of about 23%. To contribute to the improvement of the energy performance of bioclimatic habitats in hot and humid climatic zones, (Camara et al., 2018) studied the thermal behaviour of habitats in local and modern materials. They found that for similar types of housing, constructions made of local materials (earthen materials) offer a better indoor thermal atmosphere compared to modern constructions (cement blocks). (Chahwane et al.,2012) have shown that the thermal inertia of building envelope materials, when taken into account from the design stage, is a major asset for storing free intakes during the day and the restitution later in hot climates given the importance of the day/night variation in the outside temperature and the potential for night-time ventilation.

The originality of the present work lies in the fact that it develops construction systems based on local building materials to improve thermal comfort in buildings, without the need for active air conditioning. this work focuses on the use of plant fibres (reed, Typha and straw) in the design of lightweight roofs on different walls to improve thermal comfort and reduce energy consumption. This work aims to contribute to improving thermal comfort in the buildings through the judicious choice of local bio-sourced or geo-sourced building materials in the development of construction systems, on the one hand, and to reduce the carbon footprint, especially operational carbon, which corresponds to all the emissions from all the energy sources used for the building's energy needs, on the other hand

## 2. METHODOLOGY

### 2.1 Description of the building model

The simulated building is a single-zone structure with 16m² of living space and a height of 3m, built on an earth platform with two windows and a wooden door on the south-facing facade. The windows measure 1.2m x 1.4m and the door 1.1m x 2.1m. The walls of the building are 3 m high, 15 to 20 cm thick and covered with cement plaster 2 cm thick or not, depending on the type. It is assumed that the windows and door remain open between 6 am and 6 pm, and the rate of air exchange in the building is considered and described by an additional term added to the heat balance equation governing heat transfer in the building. In this investigation, six lightweight roofs and five envelopes were modelled. First without insulation, then with a thermal insulation system. The temperatures of the air inside the building, the four internal walls, the floor, the wooden ceiling and the external roof were simulated and compared in terms of thermal comfort. Figure 1 illustrates the descriptive diagram of the different modes of heat exchange in the habitable envelope.

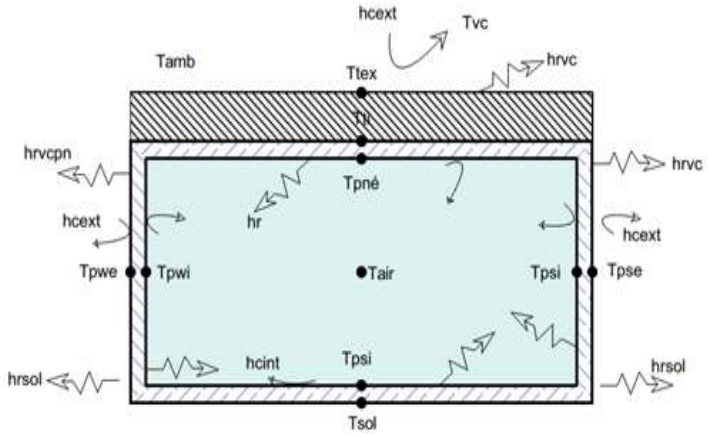


**Figure 1. Descriptive diagram of the different modes of heat exchange in the living building envelope**

**Table 1. Thermo-physical properties of housing materials (Fohaguiet al., 2018, Jannot et al., 2012 , Guide des matériaux pour l'isolationthermique (free.fr)).**

| Materials | Material Thermalconductivity K (W/m/K) | Density $\rho$ (Kg/m3) | Heat capacity Cp (J/Kg/K) |
|---|---|---|---|
| Sheet metal | 50 | 7800 | 450 |
| Tile | 1.73 | 2243 | 920 |
| Straw | 0.065 | 100 | 2000 |
| Reed | 0.055 -0.09 | 120 -255 | 1400 -2000 |
| Typha | 0.03319 | 360 | - |
| Banco | 0.5 -1.5 | 1600 -1900 | 600 -1000 |
| Stone | 1.4 | 1895 | 1000 |
| Wood | 0.15 | 1200 | 480 |
| Stabilized earth brick (SEB) | 1.1 | 1500 | 2000 |
| Breezeblock | 0.833 | 1000 | 1000 |
| slab | 1.4 | 1001 | 2300 |
| Terra cotta | 1-1.35 | 1700 -2100 | - |
| Granite | 2.8 | 2600 | 1000 |
| Cement plaster | 1.4 | 2240 | 840 |
| Coconut fibre | 0.037 -0.047 | 20 - 60 | 1500 -1800 |
| Sheep wool | 0.035 -0.045 | 13 -35 | 1000 -1800 |
| Wood wool | 0.035 - 0.045 | 35 - 50 | 1600 - 2300 |

## 2.2 Mathematical formulation

The methodology adopted for the description of the thermal behaviour of our habitat model is based on the nodal analysis used by (Boyer et al., 2001) and (Thomas Nganyaa et al., 2012). The detailed study of the heat transmission phenomena involved in the functioning of the habitat (Figure 1)

### 2.2.1. Basic Energy transfer

The equations of transfer are based on the analogy between heat and electrical transfers. Generally speaking, the instantaneous change in energy within a habitat component equals the algebraic sum of the flux densities exchanged within that component. It is written:

$$\frac{M_i C_{P_i} \partial T_i}{s\ \partial t} = \mathrm{DFS}A_i + \sum_{i=1}^{n} \sum_x h_{xij}\,(T_j - T_i) \quad (1)$$

$\varphi_{xij}$ is the heat flux density exchanged by the transfer mode x (conduction, convection, and radiation) between media (i) and (j) (w.m$^{-2}$);

- s is the cross-section of the wall in (m$^2$);
- DFS$A_i$, the density of solar flux absorbed by the material (i).

DFS$A_i$= $\alpha_i \varphi_i$

- $\alpha_i$is the heat absorption coefficient of the material

$\varphi_i$ Solar flux density captured by the surface of the medium (i) (w.m$^{-2}$) By introducing a $h_{xij}$ exchange coefficient and linearizing the transfers, we can write

$\varphi_{xij} = h_{xij}(T_j - T_i)$
(3)
Thus equation (1) is written:
$\frac{M_i C_{P_i} \partial T_i}{s \ \partial t} = \alpha_i \varphi_i \ + \sum_{i=1}^{n} \sum_x h_{xij} \ (T_J - T_i)$
(4)
Equation (4) is applied to the various walls and roofs of the systems studied.

### 2.22 *Equations Simplifying assumptions*

The heat transfer model adopted in the building is a 1D transient model which represents the main heat transfers on the different walls of the building. The heat transfer equations are written at the level of each construction system considered. Each wall is subdivided into two identical isothermal nodes. The notion of perfect contact is taken into account for adjacent elements. The energy transfer equations for the walls or roofs of the house are written using the analogue electrical diagram. Each roof or wall envelope is associated with two nodes for which heat balances are performed. The equations obtained are then discretized in the direction transverse to the heat transfer fluid flow using the implicit finite difference method.
Heat transfer is unidirectional, the thermal inertia of the air is negligible, the materials are assimilated to grey bodies, the air renewal rate is variable within the building enclosure; the heat transfer fluid is assumed to be a perfect and incompressible gas, the thermo-physical properties of the materials are assumed to be constant and independent of temperature, the ambient temperature and sunshine are instantaneous functions on all the surfaces of the walls and roofs.

### 2.3 Energy transfer equations

The transfer equations are based on the analogy between thermal and electrical transfers. Generally speaking, the instantaneous variation in energy within a housing component equals the algebraic sum of the flux densities exchanged within this component.
Energy transfer equations at rooftop
The exterior wall of the rooftop
$\frac{M_{tex} C_{P_{tex}}}{S} \frac{\partial T_{tex}}{\partial t} = \alpha_{tex} \varphi_{tex} + \frac{K_{tex}}{E_{p_{tex}}} (T_{ti} - T_{tex}) + h_{c_{ex}} (T_{air} - T_{tex}) + h_{r_{vc,tex}} (T_{vc} - T_{tex}) + h_{r_{sol,tex}} (T_{sol} - T_{tex})$ (5)
The internal wall of the roofto
$\frac{M_{ti} C_{P_{ti}}}{S} \frac{\partial T_{ti}}{\partial t} = \frac{K_{ti}}{E_{p_{ti}}} (T_{tex} - T_{ti}) + h_{c_1} (T_{air} - T_{ti}) + h_{r_{ti,pni}} F_{ti,pni} (T_{pni} - T_{ti}) + h_{r_{ti,psi}} F_{ti,psi} (T_{psi} - T_{ti}) +$
$h_{r_{ti,pei}} F_{ti,pei} (T_{pei} - T_{ti}) + h_{r_{ti,pwi}} F_{ti,pwi} (T_{pwi} T_{ti})$ (6)

Governing equations at the building level
Establishing a heat balance at each node associated with the transfers in the habitat model leads to the following transfer equations.
The north External wall of the building
$\frac{M_{pnh} C_{p_{pnh}}}{S} \frac{\partial T_{pne}}{\partial t} = \alpha_{pne} \varphi_{pne} + \frac{K_{pnh}}{E_{pnh}} (T_{pni} - T_{pne}) + h_{c_{ex}} (T_{air} - T_{pne}) + h_{r_{vc,pne}} (T_{vc} - T_{pne}) + h_{r_{sol,pne}} (T_{sol} -$
$T_{pne})$ (7)

The north internal wall of the building
$\frac{M_{pnh} C_{p_{pnh}}}{S} \frac{\partial T_{pni}}{\partial t} = \frac{K_{pnh}}{E_{pnh}} (T_{pne} - T_{pni}) + h_{c_{pni}} (T_{airh} - T_{pni}) + h_{r_{pni,pipl}} F_{pni,pipl} (T_{pipl} - T_{pni}) + h_{r_{pni,psi}} F_{pni,psi} (T_{psi} -$
$T_{pni}) + h_{r_{pni,pei}} F_{pni,pei} (T_{pei} - T_{pni}) + h_{r_{pni,pwi}} F_{pni,pwi} (T_{pwi} - T_{pni})$
(8)
Indoor air in the building
$\frac{M_{air} C_{p_{air}}}{S} \frac{\partial T_{airh}}{\partial t} = h_{c_{pni}} (T_{pni} - T_{airh}) + h_{c_{psi}} (T_{psi} - T_{airh}) + h_{c_{pei}} (T_{pei} - T_{airh}) + h_{c_{pwi}} (T_{pwi} - T_{airh}) + h_{c_{ti}} (T_{ti} -$
$T_{airh}) + \mathrm{CQ} \ (T_{amb} - T_{airh})$ (9)

The internal wall of the building floor

$\frac{M_{ppl} C_{p_{ppl}}}{S} \frac{\partial T_{pipl}}{\partial t} = \frac{K_{ppl}}{E_{ppl}} (T_{spl} - T_{pipl}) + h_{c_{ppl}} (T_{airh} - T_{pipl}) + h_{r_{pipl,psi}} F_{pipl,psi} (T_{psi} - T_{pipl}) + h_{r_{pipl,pei}} F_{pipl,pei} (T_{pei} -$
$T_{pipl}) + h_{r_{pipl,pwi}} F_{pipl,pwi} (T_{pwi} - T_{pipl}) + h_{r_{pipli,pni}} F_{pipl,pni} (T_{pni} - T_{pipl}) ) + h_{r_{pipli,ti}} F_{pipl,ti} (T_{ti} -$
$T_{pipl})$ (10)
The south external wall of the habitat
$\frac{M_{psh} C_{p_{psh}}}{S} \frac{\partial T_{pse}}{\partial t} = \alpha_{pse} \varphi_{pse} + \frac{K_{psh}}{E_{psh}} (T_{psi} - T_{pse}) + h_{c_{ex}} (T_{air} - T_{pse}) + h_{r_{vc,pne}} (T_{vc} - T_{pse}) + h_{r_{sol,pse}} (T_{sol} -$
$T_{pse})$ (11)

The south internal wall of the building

$$\frac{M_{psh}C_{p_{psh}}}{S}\frac{\partial T_{psi}}{\partial t} = \frac{K_{psh}}{E_{psh}}\left(T_{pse} - T_{psi}\right) + h_{c_{psi}}\left(T_{airh} - T_{psi}\right) + h_{r_{psi,pni}}F_{psi,pni}\left(T_{pni} - T_{psi}\right) + h_{r_{psi,pei}}F_{psi,pei}\left(T_{pei} - T_{psi}\right) + h_{r_{psi,pwi}}F_{psi,pwi}\left(T_{pwi} - T_{psi}\right) + h_{r_{psi,pipl}}F_{psi,pipl}\left(T_{pipl} - T_{psi}\right) \quad (12)$$

The east external wall of the building

$$\frac{M_{peh}C_{p_{peh}}}{S}\frac{\partial T_{pee}}{\partial t} = \alpha_{peh}\varphi_{peh} + \frac{K_{peh}}{E_{peh}}\left(T_{pei} - T_{pee}\right) + h_{c_{ex}}\left(T_{air} - T_{pee}\right) + h_{r_{vc,pne}}\left(T_{vc} - T_{pne}\right) + h_{r_{sol,pne}}\left(T_{sol} - T_{pee}\right) \quad (13)$$

The east internal wall of the building

$$\frac{M_{peh}C_{p_{peh}}}{S}\frac{\partial T_{pei}}{\partial t} = \frac{K_{peh}}{E_{peh}}\left(T_{pee} - T_{pei}\right) + h_{c_{pei}}\left(T_{air} - T_{pei}\right) + h_{r_{pei,pni}}F_{pei,pni}\left(T_{pni} - T_{pei}\right) + h_{r_{pei,pwi}}F_{pei,pwi}\left(T_{pwi} - T_{pei}\right) + h_{r_{pei,psi}}F_{pei,psi}\left(T_{psi} - T_{pei}\right) + h_{r_{pei,pipl}}F_{pei,pipl}\left(T_{pipl} - T_{pei}\right) \quad (14)$$

The west external wall of the building

$$\frac{M_{pwh}C_{p_{pwh}}}{S}\frac{\partial T_{pwe}}{\partial t} = \alpha_{pew}\varphi_{pew} + \frac{K_{pwh}}{E_{pwh}}\left(T_{pwi} - T_{pwe}\right) + h_{c_{ex}}\left(T_{air} - T_{pwe}\right) + h_{r_{vc,pwe}}\left(T_{vc} - T_{pwe}\right) + h_{r_{sol,pwe}}\left(T_{sol} - T_{pwe}\right) \quad (15)$$

The west internal wall of the building

$$\frac{M_{pwh}C_{p_{pwh}}}{S}\frac{\partial T_{pwi}}{\partial t} = \frac{K_{pwh}}{E_{pwh}}\left(T_{pwe} - T_{pwi}\right) + h_{c_{pwi}}\left(T_{airh} - T_{pwi}\right) + h_{r_{pwi,pni}}F_{pwi,pni}\left(T_{pni} - T_{pwi}\right) + h_{r_{pwi,pei}}F_{pwi,pei}\left(T_{pei} - T_{pwi}\right) + h_{r_{pwi,psi}}F_{pwi,psi}\left(T_{psi} - T_{pwi}\right) + h_{r_{pwi,pipl}}F_{pwi,pipl}\left(T_{pipl} - T_{pwi}\right) \quad (16)$$

## 2.4. Numerical study

The systems of algebraicequationsobtained by establishing the energy balances on the different components of the habitat model are of the form(Boyer et al., 2001, Dalel,M., 2010)

$$C\frac{d\,T(t)}{dt} = -\,K.T(t) + B.G(t) \quad (17)$$

With T(t): the state vector of the temperatures at the different time-dependent nodes t, C: the column vector of the heat capacities at the different nodes, K: the square matrix composed of the thermal conductances, B: the matrix coefficient for the different nodes, G(t): the column vector representing the inputs to the system. Equations (5 to 16) are discretized by an implicit finite difference method; This method is based on a Taylor series expansion that transforms partial differential equations into a system of algebraic equations that requires iterative computation to solve. The system is solved by the iterative method of Gauss-Seidel.

At the initial time $t_o$, the different temperatures of all wall walls and roofs are assumed to be equal to the ambient temperature. At the time $t_o+\Delta t$, a new value of the temperatures of the system components is calculated. The solution of the system of algebraic equations (5 to 16) leads to new temperature values that are compared to the arbitrary value initially chosen. If the difference between these two consecutive temperatures is greater than the desired accuracy, the calculated temperature values override the arbitrary value and the procedure described above is repeated until convergence is achieved. Convergence is achieved when the following criterion is met:$\frac{T^{t+\Delta t}-T^{t}}{T^{t+\Delta t}} \leq 10^{-5}$

## 2.5 Material and Methodology

The tools we use for this research are the Lomé climatic data for a typical day in March with a global irradiance of 700W/m², the maximum and minimum values of the ambient temperature being 33°C and 26°C respectively. These data enable us to find the hourly variations in ambient temperature and solar flux by considering a sinusoidal variation (Figure 1).

The programming language is Fortran 95 and the Origin software is used to draw the curves. Figure 2 shows the evolution of global solar radiation on a horizontal plane (RGH) and the ambient temperature (Tamb) for a typical day in March (16th March 2022), the hottest day of the year. We have therefore chosen the climatic data for this typical day as the input data for our program, as it enables us to analyze the thermal behaviour of the home under Lomé extreme climatic conditions.

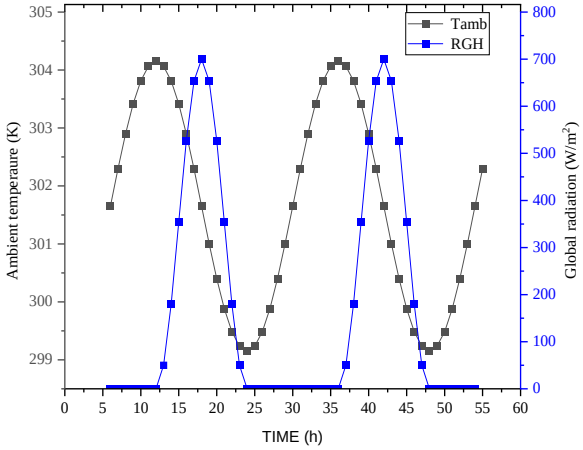


**Figure 2. Overall sunshine and ambient temperature on a typical day in March (16th March 2022)**

## 3.RESULTS AND DISCUSSION

### 3.1 model validation

We have chosen to validate by literature data on our model based on a numerical study of the thermal comfort of a similar bioclimatic building carried out by (Camara et al., 2018). Figure 2 shows the evolution of the temperature profile of the external (Ttext) and internal (Ttint) walls of the roof of a bioclimatic building. The roof is considered to be a flat wall with a rectangular cross-section and an angle of inclination of 30° to the horizontal, made up of sheets of 8 mm thick aluminium sheeting and vertical walls of stabilized earth bricks (SEB) in which air circulates by convection. Figure 2 shows that the curves obtained by the present work in terms of external and internal rooftop temperatures are quantitatively and qualitatively consistent with those obtained by (Camara et al., 2022) in similar conditions.

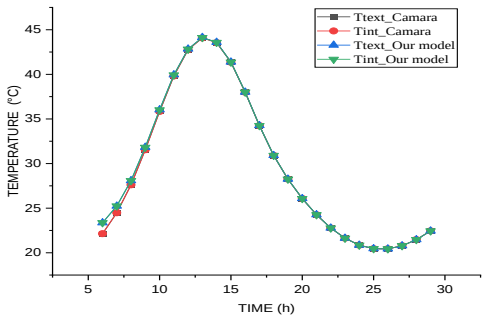


**Figure 3. Model validation**

### 3.2 Temperature distribution in lightweight roof buildings

#### 3.2.1 Building with Banco Walls

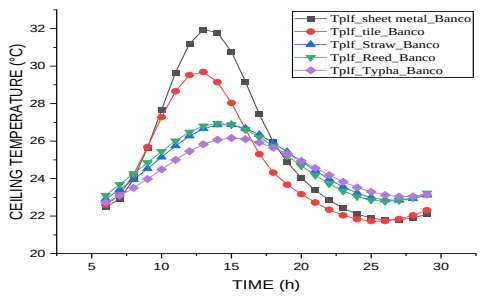


**Figure 4. Variation in indoor air temperature as a function of lightweight roofs on a banco wall building**

Figure 4 shows the evolution, over time, of the temperature of the air inside the building (Tairh) made of banco with five different roofs (sheet metal, tile, straw, reed and Typha). For these construction systems, sheet metal and roof tiles provided maximum temperatures of 32.4°C and 31.2°C respectively at 2 pm, while plant fibres such as straw, reed and Typha provided a thermal environment of 29.85, 29.80 and 29.60°C respectively at 3 pm; these temperatures are acceptable in terms of thermal comfort for a dry, humid tropical zone in sub-Saharan Africa. Earth construction systems with lightweight plant-fibre roofs always offer better thermal comfort than modern materials. These results are to be expected and are consistent with (Kemajou et al., 2012). Figures (5 to 6) show respectively the evolution of the temperature profiles of the lower surface of the wooden ceiling (Tplf) and the floor (Tpl) for five different plant fibre roofing systems (sheet metal, tile, straw, reed and Typha) on a banco wall building. It can be seen that plant fibre roofs offer comfortable temperatures compared with conventional sheet metal and tile roofs. There is a difference in temperature around 6°C between sheet metal and Typha. This can be explained by the thermo-physical properties of these plant fibres, which are practically regarded as thermal insulators. Typha roofs are also highly effective at regulating the temperature inside the building. Typha is a naturally insulating material that offers excellent protection against the heat in summer and the cold in winter. On the other hand, roofs made of sheet metal, tiles tend to absorb heat and retain it, which can make the inside of the building very hot during hot periods. They also tend to be less insulating than straw or typha roofs. The temperature distribution at the floor level of the building with a conventional roof (sheet metal and tiles) is slightly higher than that of the straw, reed or Typha roofs. It can be seen that temperatures are lower at floor level than for the other components of the habitat (difference of 0.75°C between sheet metal and Typha).

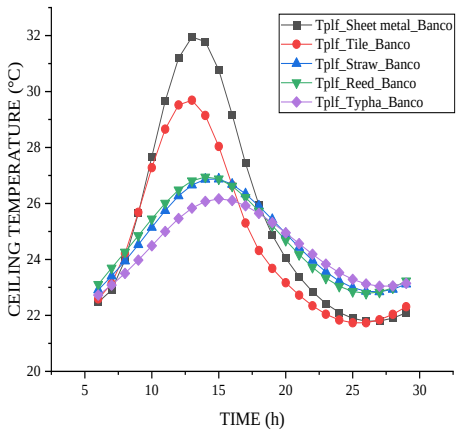


**Figure 5. Variation in ceiling temperature as a function of lightweight roofs on a banco wall building**

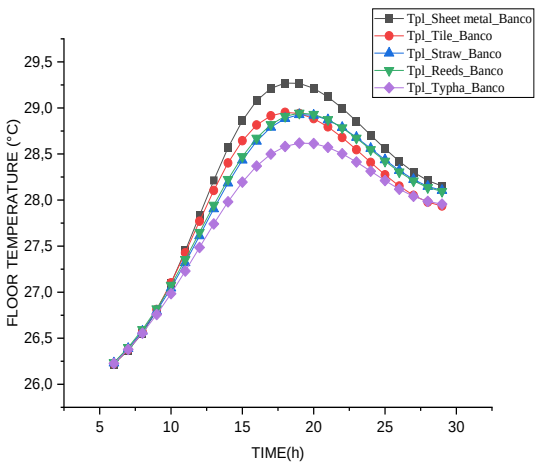


**Figure 6. Variation in floor temperature as a function of lightweight roofs on a banco wall building**

Figures 7 (a - d) show respectively the evolution of the temperature profiles of the interior walls for five different plant fibre roofing systems (sheet metal, tile, straw, reed and Typha) on a banco wall building. The

south and north interior walls show the lowest temperatures (26.2 to 27.5°C and 24.6 to 25.8°C respectively), Figure 7 (a - b), while those of the east and west interior walls are relatively high (27 to 28.5°C and 28 to 29°C respectively), Figure 7(c- d). This can be explained by the fact that the east and west walls are the most exposed to incident solar radiation, while the north and south walls receive relatively little solar radiation.

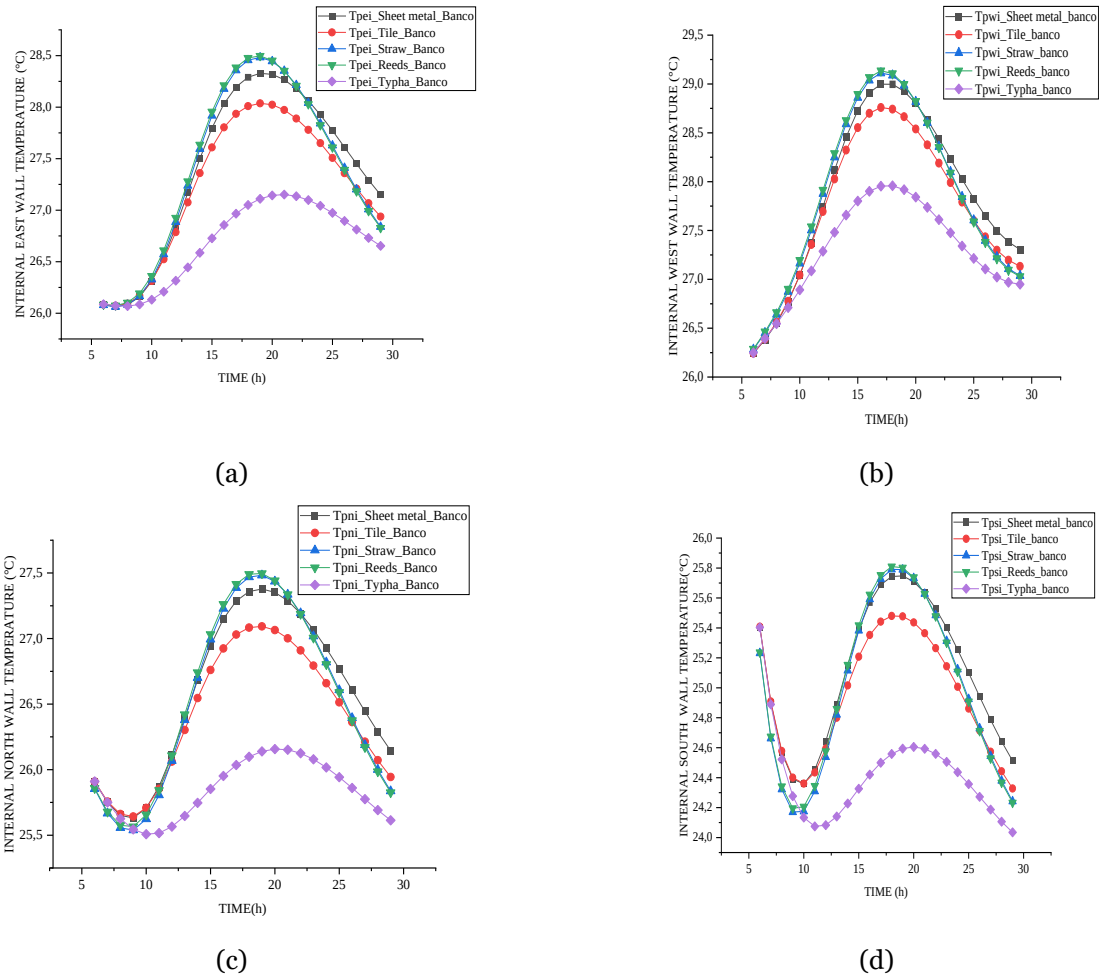


**Figure 7. Variation in internal wall temperature as a function of lightweight roofs on a banco wall building: a) East interior; b) West interior; c) North interior; d) South interior.**

### 3.2.2 Stone Wall Building

Figure 8 shows the evolution of the indoor air temperature of the stone habitat (Tairh) covered with five different roofing systems (tin, tile, straw, reed and Typha).

For these systems, sheet metal and tiles give maximum temperatures of 32.7°C and 31.4°C respectively at 3 p.m., while straw fibre, reed and Typha roofs give temperatures of 31, 31 and 30°C respectively at 3 p.m. Stone buildings covered with plant fibres have a better thermal environment than buildings made of cement blocks topped with metal sheeting in the dry, humid tropics of sub-Saharan Africa (Mba, 2011)

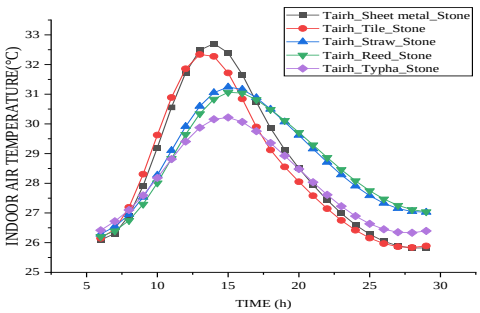


**Figure 8. Variation in indoor air temperature as a function of light roofs on a stone wall building**

### 3.2.3 Wooden Wall Building

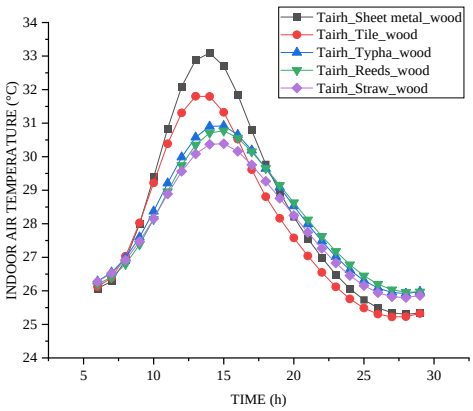


**Figure 9. Variation in indoor air temperature as a function of lightweight roofing on a timber building.**

Figure 9 shows the change in indoor air temperature in a wooden dwelling (Tairh) with five different roofing systems (tin, tile, straw, reed and Typha). For these systems, sheet metal and tile roofs gave maximum temperatures of 33°C and 31.8°C respectively at 3 pm, while straw fibre, reed and Typha roofs gave temperatures of 30.9, 30.8 and 30.4°C respectively at 3 pm. Building systems made of wood topped with plant fibres have a better thermal environment than those made of modern materials in the dry and humid tropics of sub-Saharan Africa (Kemajou et al., 2012).

### 3.2.4 Building with stabilized earth brick (SEB) walls

Figure 10 shows the evolution of the temperature of the air inside the building (Tairh) in SEB capped with five different roofs (sheet metal, tile, straw, reed and Typha). For these systems, sheet metal and tile roofs gave maximum temperatures of 33°C and 32.5°C respectively at 3 pm, while straw fibre, reed and Typha roofs gave temperatures of 31.2, 30.1 and 30°C respectively at 3 pm. Buildings made of stabilized earth brick and raw earth covered with plant fibres have a better thermal performance than those made of breeze blocks covered with sheet metal in the dry and humid tropical zones of sub-Saharan Africa (Kemajou et al., 2012). One can conclude that Typha is a naturally insulating material that offers excellent protection against the heat in the hot or cold period in the building.

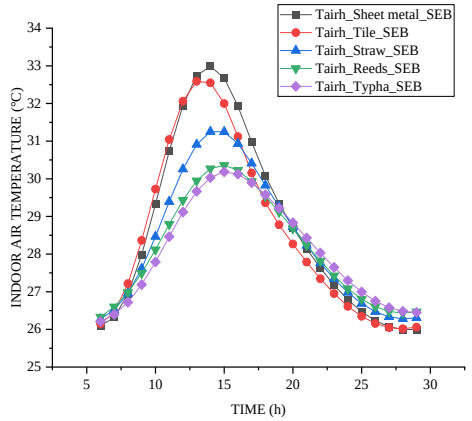


**Figure 10. Variation in the temperature of the air inside the building as a function of lightweight roofs on a SEB wall building**

Figure 11 shows the change in indoor air temperature in the habitat (Tairh) in a cement block wall topped with four different roofs (sheet metal, tile, straw and Typha). For these systems, the sheet metal and tile roofs gave maximum temperatures of 37°C and 36.5°C respectively at 3 pm, while the straw fibre and Typha roofs gave maximum temperatures of 33°C and 33.5°C respectively at 3 pm. Sheet metal and breeze-block walls allow a large proportion of the heat to spread inside the home, creating conditions of thermal discomfort.

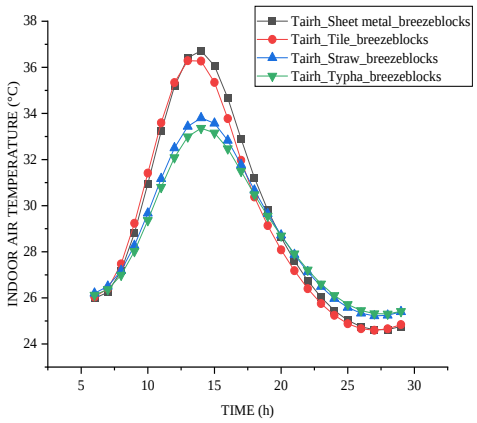


**Figure 11. Variation in indoor air temperature as a function of lightweight roofs on a cement block wall building**

### 3.3 Improving thermal comfort by designing the walls of buildings with lightweight roofs

#### 3.3.1 Wall of different materials

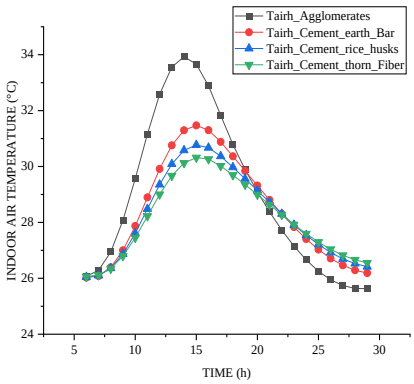


**Figure 12. Variation of the indoor air temperature of the habitat as a function of different walls under a lightweight roof (tin roof)**

Figure 12 shows the evolution of the indoor air temperature in the habitat (Tairh) with four different walls (chipboard wall, cement wall with rice husks, cement wall with bar soil and cement wall with roast tree fibres). The maximum temperatures observed were 34°C and 31°C at 3 pm for the chipboard and cement with bar soil walls respectively. The lowest temperatures recorded were 30.1°C and 30.2°C at 3 pm. respectively for the walls made of cement with roast wood fibre and cement + rice husks. The air temperature in the building depends on the main construction materials. The relatively low temperatures noted for walls made of cement + rice husks and cement with bar soil can be explained by the fact that these composites have a fairly low conductivity coefficient and a high thermal heat capacity. The same is true for cement withbar soil walls compared with chipboard walls. These results are consistent with the results of studies carried out by several authors and reported in the literature (Gbaguidi et al., 2011, Godonou et al., 2022). Figure 13 shows the evolution of the indoor air temperature profile of the tin-roofed habitat (Tairh) with four different walls (breeze-block wall, breeze-block wall with 2 cm cement render insulation, double-skin breeze-block terra cotta wall and double-skin breeze-block granite wall). The maximum temperatures observed were 37°C and 36°C at 3 pm for the breeze-block walls and the breeze-block wall with cement rendering insulation respectively. The lowest temperatures recorded were 31.8°C and 32.5°C at 3 pm for the double-skin granite breeze-block and double-skin clay breeze-block walls respectively. The temperature of the air in the home depends on the main construction materials, but also on the inertia of the walls. The relatively low temperatures noted for walls made of cement with rice husks and cement with bar soil can be explained by the fact that these composite walls have a fairly low conductivity coefficient and a high specific heat capacity. The thermal inertia of the walls of double-skinned buildings is higher than that of single-wall housing, which slows the transfer of heat from the outside to the inside of the building and consequently reduces thermal discomfort inside the building.

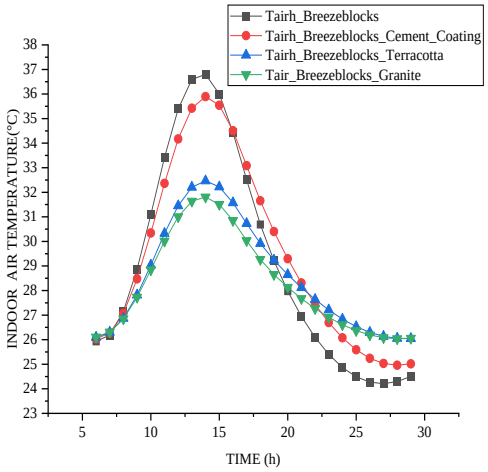


**Figure 13. Variation in indoor air temperature of zinc sheet roofing habitat as a function of different building walls**

### 3.3.2 Insulation of external walls

Figure 14 shows the evolution over time of the indoor air temperature of the cement breeze-block (PRG) walls covered with tiles for five different insulation cases (PRG, coconut fibre, sheep's wool, straw bales and wood wool). For these five cases, there is a difference of 6°C between the insulated and non-insulated systems (temperatures drop from 37°C to 30°C). The introduction of insulation significantly reduces the temperature inside the building.

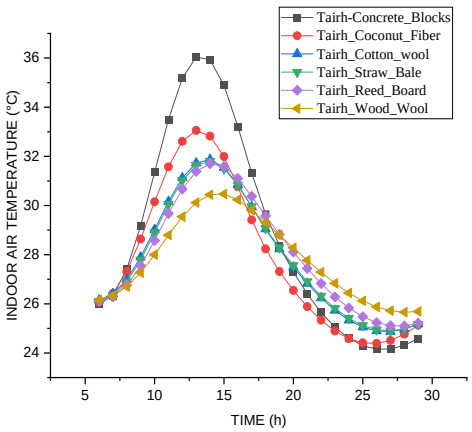


**Figure 14. Variation in indoor air temperature in a cement block wall building covered with a sheet metal roof as a function of the building's walls**

## 4. CONCLUSION

This paper presents the main results of a study based on the use of local building materials to improve thermal comfort in buildings constructed using these local materials. The aim was to predict indoor air and building wall temperatures by simulating the latter in a sub-Saharan climate zone. Emphasis was placed on the importance of insulation in lowering indoor temperatures in conventional housing. Lightweight roofs made of straw, Typha, reed, sheet metal and tiles, as well as walls made of banco, SEB, wood, stone and breeze-block, with and without insulation, were studied. The results of the simulations show, on the one hand, the considerable impact of using local materials in building construction on reducing interior and wall temperatures by up to 15%, and on the other hand the positive influence of insulation on reducing heat flow and therefore temperatures by up to 17%. One can conclude that:

- Stone buildings covered with plant fibres have better thermal comfort than buildings made of cement blocks topped with metal sheeting in the dry, humid tropics of sub-Saharan Africa;
- earth construction systems with lightweight plant-fibre roofs always offer better thermal comfort than modern materials;

- The temperature of the air in the room depends on the main construction materials, but also on the inertia of the walls;
- building systems made of wood topped with plant fibres have better thermal comfort than those made of modern materials in the dry and humid tropics.

These results open up several avenues for future research, in particular the massive physical and mechanical characterization of local building materials for large-scale use.

## REFERENCES


1. Allouhi, A., El Fouih,Y., Kousksou, T., Jamil, A., Zeraouli, Y., and Mourad, Y. "Energy consumption and efficiency in buildings: Current status and future trends," J. Clean. Prod., vol. 109, pp. 118–130, 2015, doi: 10.1016/j.jclepro.2015.05.139.
2. Aek, H. "Etude thermiqued'unemaisontraditionnelleenAlgérie, cas de Oued Souf," vol. 31, pp. 19–23, 2017.
3. Bastide, A., Boyer, H., Lauret, P., Lucas, F., and Garde, F. "Intégration {à} TRNSYS du noyau de CODYRUN, code de simulation thermo-aéraulique de bâtiments : le Type 59," 4ième séminaire TRNSYS-EES, pp. 1–6, 2001, [Online]. Available: https://hal.archives-ouvertes.fr/hal-00768184
4. Benamara, D. and Mezghiche, B. "Vers Un Beton De Haute Performance Elabore De MateriauxLocaux « Bhp »," Courr. du savoir, vol. 10, pp. 9–14, 2010.
5. Betti, G., Tartarini, F., Nguyen C., and Schiavon, S. "CBE Clima Tool: A free and open-source web application for climate analysis tailored to sustainable building design," Build. Simul., vol. 17, no. 3, pp. 493–508, 2024, doi: 10.1007/s12273-023-1090-5.
6. Boukli Hacene, M. A., Amara, S., and Chabane Sari, N. E. "Thermal requirements and temperatures evolution in an ecological house," Energy Procedia, vol. 6, pp. 110–121, 2011, doi: 10.1016/j.egypro.2011.05.013.
7. Chahwane, L. "Valorisation de l 'inertiethermique pour la performance énergétique des bâtiments To cite this version: HAL Id: tel-00701170 Valorisation de l ' inertiethermique pour la performance énergétique des bâtiments," 2012.
8. Camara Y. and Chesneau, X. "Étude numérique du confortthermique dans un habitat bioclimatiqueenbrique de terre stabilisée pour un climat type de la Guinée," vol. 14, no. 2, pp. 238–254, 2018.
9. Camara Y. and Chesneau, X. "Étude numérique du confortthermique dans un habitat bioclimatiqueenbrique de terre stabilisée pour un climat type de la Guinée," vol. 14, no. 2, pp. 238–254, 2018.
10. Camara, Y., Ouedraogo, D., Sawadogo, L. G. and Compaore, A. "Comparative Study of the Thermal Performance of three pitched Roof Models for a Humid Tropical Climate: case of Guinea," vol. 13, no. 7, pp. 791–803, 2022.
11. Cheung, C. K., Fuller, R. J. and Luther, M. B. "Energy-efficient envelope design for high-rise apartments," vol. 37, no. May 2004, pp. 2004–2006, 2005, doi: 10.1016/j.enbuild.2004.05.002.
12. Dalel, M. "Modélisation de l' impact de l' isolation thermique sur la températureintérieure," Séminaire Int. sur le Génie Clim. l'Energétique, SIGCLE'2010, vol. 13, pp. 265–273, 2010.
13. Fezzioui, N. and Larbi, M. B. S. "Influence des caractéristiquesdynamiques de l 'enveloppe d' un bâtiment sur le confortthermique au sudAlgérien," vol. 11, pp. 25–34, 2008.
14. Fohagui, F. C. V., Koholé Y. W., and Tchuen, G. "Experimental comparison of energy performances of common types of buildings constructed in Cameroon and validation of their electrical model," Sadhana - Acad. Proc. Eng. Sci., vol. 46, no. 3, 2021, doi: 10.1007/s12046-021-01670-9.
15. Gbaguidi, V., Gbaguidi, A., Gibigaye, M., Adjovi, E., Sinsin, B. and Amadji, T., "Determination experimentale des principalescaracteristiques physiques et mecaniques du bois du rônier (borassusaethiopum Mart.) d'originebeninoise," J. la Rech. Sci. l'Universite Lome, vol. 12, no. 2, 2011, doi: 10.4314/jrsul. v12i2.68046.
16. Gibigaye, M., Godonou, F. G., Yabi, C. P. and Degan, G. "Estimation of Elastic Properties of Oil Palm Kernel Shell Concrete by Semianalytical Methods of Homogenisation," Adv. Civ. Eng., vol. 2019, 2019, doi: 10.1155/2019/9256260.
17. Guiavarch Alain, "Etude de l'amélioration de la qiualité environnementale du batiment par intégration de composant solaire," Thèse de Doctorat soutenu en 2003 à l'Université Cergy-Pontoise
18. '' Guide des matériaux pour l ' isolation thermique".Guide des matériaux pourl'isolation thermique Guide des matériaux pour l'isolationthermique (free.fr) en ligne
19. Institut de la Francophonie pour le Développement Durable (IFDD), Conception Architecturale Durable En Milieu Tropical Conception Architecturale. 2015. [Online]. Available: www.ifdd.francophonie.org
20. Jannot Y. and Djiako, T. "Economied'énergie et confortthermique dans l'habitaten zone tropicale," Int. J. Refrig., 1994, doi: 10.1016/0140-7007(94)90015-9.

21. Jannot, Y."Un procédé économique pour l ' amélioration du confort thermique en zone tropicale sèche : la ventilation par de l ' air extérieur éventuellement humidifié," 2019. Rev. Int. Froid 1994 Volume 17 Numéro 3 PP 175-179
22. Jannot ,Y. and A. Degiovanni. Modélisation des propriétésthermomécaniques effectives de dépôtsélaborés par projection thermique. Université de Technologie de Belfort-Montbeliard Ecole Doctorale Sciences pour l'Ingénieur et Microtechniques. Thèse de Doctorat, soutenue le 20 septembre 2012
23. Kaboré, A. "Modélisationhygrothermique de l'enveloppe du bâtiment avec le matériau de chanvre," pp. 1–252, 2020.
24. Kachkouch, S. "Évaluation expérimentale et par simulation des performances thermiques de techniques passives appliquées aux toitures pour le rafraîchissement des bâtimentsenclimatchaud Salah Kachkouch To cite this version: HAL Id: tel-02120781," Thèse Dr., no. Cotutelle à l'Université Cadi Ayyad (Maroc) et l'Université de La Rochelle (France) pour, p. 122, 2019.
25. Kemajou A., and Mba, L. "Real impact of the thermal inertia on the" Int. J. Res. Rev. ..., vol. 11, no. June, pp. 358–367, 2012, [Online]. Available: http://www.arpapress.com/Volumes/Vol11Issue3/IJRRAS_11_3_02.pdf
26. LAWSON, F. "Evaluation du confortthermique dans l'habitatindividuel à Ouagadougou,". http://documentation.2ie-edu.org. EIER Ougadougou.
27. Maamar, H. "Choix de l'orientation des Matériaux de Construction en Vue d'Améliorer les performances Thermiques des batiments," Fitzpatrick's Dermatology, vol. 53, no. 9, pp. 1779–1791, 2019.
28. Mba, A. K. L. "Matériaux de construction et confortthermiqueen zone chaude Application au cas des régionsclimatiquescamerounaises," vol. 14, pp. 239–248, 2011.
29. Medjelakh, S. and Abdou, D. "Impact de l'inertiethermique sur le conforthygrothermique et la consommationénergétique du bâtiment," Rev. des Energies Renouvelables Vol 11 N°3, 2008.
30. Nganya, T., Ladevie, B. Kemajou, A. and Mba, L. "Elaboration of a bioclimatic house in the humid tropical region: Case of the town of Douala-Cameroon," Energy Build., vol. 54, pp. 105–110, 2012, doi: 10.1016/j.enbuild.2012.07.025.
31. O. I. de la francophonie (OIF) I. de la Francophonie, Guide du bâtiment durable enrégionstropicales. Tome 1. 2015.
32. Samah, H.-A., Banna, M. and Zeghmati, B. "Double Diffusive Convection Heat and Moisture Transfer Inside a Planted Roof Building Under Hot Humid Climate: Case of Lomé City in West Africa," Am. J. Appl. Sci., vol. 19, no. 1, pp. 6–20, 2022, doi: 10.3844/ajassp.2022.6.20.
33. Ullah, K. R., Prodanovic, V., Pignatta, G., Deletic, A. and Santamouris, M. "Assessing the impact of heat mitigation measures on thermal performance and energy demand at the community level: A pathway toward designing net-zero energy communities," Build. Simul., no. Santamouris 2015, 2024, doi: 10.1007/s12273-024-1140-7.


## Nomenclature

h_rsol: Wall-to-soil radiation transfer coefficient ($W.m^{-2}.K^{-1}$)

h_rvc: Wall-to-Earth Radiation Transfer Coefficient ($W.m^{-2}.K^{-1}$)

K: Thermal conductivity ($W.m^{-1}.K^{-1}$)

h_cex: Transfer coefficient by convection from the outside wall ($W.m^{-2}.K^{-1}$)

hr_(i→pi): Radiation transfer coefficient between other walls ($W.m^{-2}.K^{-1}$)

α_tex: Absorption coefficient of the external covering (constant)

φ_tex: Heat flux density at the external wall ($W.m^{-2}$)

h_rsol: Wall-to-soil radiation transfer coefficient ($W.m^{-2}.K^{-1}$)

h_rvc: Wall to celestial crust radiation transfer coefficient ($W.m^{-2}.K^{-1}$)

K: Thermal conductivity ($W.m^{-1}.K^{-1}$)

h_cex: Transfer coefficient by convection from the outside wall ($W.m^{-2}.K^{-1}$)

hr_(i→pi): Radiation transfer coefficient between other walls ($W.m^{-2}. K^{-1}$)

α_tex: Absorption coefficient of the external covering (constant)

φ_tex: Heat flux density at the external wall ($W.m^{-2}$)

ϕ_ra: Exchange flux per air change ($J.h^{-1}$)

T_tex: External roof temperature (k)

T_int: Internal roof Temperature (k)

T_pni: Temperature of the internal north wall (k)

T_pne: erature of external north wall (k)

T_psi: Temperature of the internal south wall (k)

T_pse: Temperature of the external south wall (k)

T_pwi: Temperature of the internal west wall (k)

T_pwe: Temperature of the external West wall (k)

T_pei: Temperature of the internal east wall (k)

T_pee: Temperature of the external east wall (k)

T_airh: Indoor air temperature (k)

T_plf: Wood ceiling temperature (k)

T_pl: Floor temperature (k)

Q: Air flow rate ($m^3$ /h)

C: Heat density of the air (C =1225 $m^3$/K)

t:

T(t): The state vector of time-dependent temperatures at the various nodes

C: Acolumn vector of thermal capacities at the various nodes

B: Matrix coefficient for the different nodes

G(t): Column vector representing system inputs